A&A manuscript no.
(will be inserted by hand later)

Your thesaurus codes are:
06 (02.01.2; 08.02.1: 08.02.3; 08.09.2: 13.25.5)

ASTRONOMY AND ASTROPHYSICS

RX J0537.7–7034: The shortest-period supersoft X-ray source ⋆

J. Greiner[1], **M. Orio**[2], **and R. Schwarz**[1]

[1] Astrophysical Institute Potsdam, An der Sternwarte 16, D-14482 Potsdam, Germany
[2] Osservatorio Astronomico di Torino, Strada Osservatorio 20, I-10125 Pino Torinese (TO), Italy

Received 18 October 1999; accepted 14 December 1999

Abstract. We present new photometric and spectroscopic observations of the transient supersoft X-ray source RX J0537.7–7034 and find a periodicity of approximately 3.5 hrs. This establishes RX J0537.7–7034 as the supersoft X-ray source with the shortest orbital period. We furthermore derive an inclination of the binary system of $45^\circ \lesssim i \lesssim 70^\circ$, and the masses of the two binary components: $M_{accretor} = 0.6 \pm 0.2$ M$_\odot$, $M_{donor} = 0.35 \pm 0.02$ M$_\odot$. This implies that the standard scenario of supersoft X-ray sources, in which the donor is thought to be more massive than the accreting white dwarf to ensure high mass transfer rates on a thermal timescale (van den Heuvel et al. 1992), is not applicable for this system. We discuss alternative interpretations of this source as a former nova in which the thermonuclear flashes have become mild and most accreted mass is retained by the white dwarf (so-called SMC 13 type systems), or as a self-sustained wind-driven system.

Key words: X-ray: stars – accretion disks – binaries: close – stars: individual: RX J0537.7–7034, 1E 0035.4–7230 ≡ SMC 13

1. Introduction

Supersoft X-ray sources (SSS) are persistent or transient sources whose radiation is almost completely emitted in the energy band below 0.5 keV and whose bolometric luminosity is 10^{37-38} erg s^{-1} (close to the Eddington limit for a 1 M$_\odot$ star). After the *Einstein* discovery of CAL 83 and CAL 87 (Long et al. 1981, Crampton et al. 1987, Pakull et al. 1987, 1988) this class of objects was established by many ROSAT discoveries (see Orio 1995, Greiner 1996 and references therein). Several different observational facts suggest that all these very luminous sources contain white dwarfs and that many of these are burning hydrogen in a shell, with a very thin and hot atmosphere on top. The white dwarf might be single (hot PG 1159 stars or planetary nebulae nuclei, e.g. Wang 1991, Motch et al. 1993) or in a binary system. The binary supersoft X-ray sources also belong to different types with orbital periods ranging from ≃1 year for symbiotic stars down to ≃4 hours for SMC 13 type sources (Kahabka and Ergma 1997 and references therein). The subgroup with short orbital periods (≤3 days) now encompasses 9 sources in the Magellanic Clouds and the Milky Way. The widely accepted scenario for these so-called close-binary supersoft sources (CBSS) is based on a companion more massive than the white dwarf, so that mass transfer is unstable and can occur at the high rates which are required to burn the hydrogen steadily on the white dwarf surface (van den Heuvel et al. 1992, Rappaport et al. 1994). While a recent review can be found in van den Heuvel and Kahabka (1997), we remind here that supersoft X-ray sources are of great astrophysical interest also because of their possible nature as progenitors of type Ia supernovae or leading to a neutron star by accretion induced collapse.

The discovery of the supersoft X-ray source RX J0537.7–7034 was first announced by Orio & Ögelman (1993). Later Orio et al. (1997) showed that the source was transient in X-rays and appeared "on" for ≃ 1 year. Also, the optical identification with a blue variable star at $V \simeq 19.7$ mag was proposed. The optical spectrum shows the He II λ4686 line in emission and the two Balmer lines Hγ and Hδ in absorption. These spectral features appear redshifted by almost 5 Å, as is expected for a LMC membership. Finally, Orio et al. (1997) also showed that the photometric data for RX J0537.7–7034 might be consistent with a possible orbital period of only ≃ 2.5–3 hours.

Here we present new photometric and spectroscopic data of RX J0537.7–7034 that indeed prove it to have a very short period.

2. Optical photometry

We carried out new photometric observations of RX J0537.7–7034 at La Silla on January 18/19 1998 and January 24-26 1999 with the 1.5 m Danish telescope of the European Southern Observatory (ESO) equipped with the spectrograph-imager DFOSC. Observations were primar-

Send offprint requests to: J. Greiner, jgreiner@aip.de

⋆ Based on observations (60.H-0682 and 62.H-0839) obtained at the European Southern Observatory, La Silla, Chile.

Table 1. Log of all observations of RX J0537.7–7034.

Telescope/ Instrument	Date	Spectral range	No. of exposures	Duration (h)	$T_{\rm int}$ (sec)
DFOSC 1.5 m	1998 Jan 18	V/B	19/22	3.8	120/180
DFOSC 1.5 m	1998 Jan 19	V	61	2.6	120
EFOSC 3.6 m	1999 Jan 22	3800–8000 Å	7	4.2	1800
DFOSC 1.5 m	1999 Jan 24	V	74	4.0	120
DFOSC 1.5 m	1999 Jan 25	V	81	4.5	120
DFOSC 1.5 m	1999 Jan 26	V	74	2.5	120

ily done in the V band, with one run also in B. Exposure times typically were 2-3 min. each, and our total temporal coverage amounts to more than 17 hours (see details in Tab. 1). Photometric reduction in this very crowded field was done using the profile-fitting algorithm of DoPhot (Mateo & Schechter 1989). On January 24 and 25, 1999 a set of Landolt (1992) standards were observed confirming the absolute photometric calibration derived by Orio et al. (1997).

The system is very blue and has a mean magnitude and color of $V = 19.7$ mag and $B - V = -0.05$. In Fig. 1 we show the V light curves of all individual nights. The light curves of both 1998 nights and of January 26, 1999 are characterized by an overall variation of ~ 0.2 mag amplitude and rather smooth minima. In contrast, the system was much more variable on January 24 and 25, 1999 (peak-to-peak amplitude ~ 0.5 mag) and the minima appeared more asymmetric or skewed. Also, minimum light was substantially reduced down to $\sim 20^{\rm m}$.

In order to derive an orbital period we carried out a period search using the analysis-of-variance method (Schwarzenberg-Czerny 1989). The resulting periodogram (Fig. 2) shows a variety of maxima which are predominantly caused by the 1 day and 1 year sampling rates. In addition, the strong night-to-night variations of the system prevent any clear signal to emerge. The most probable periods (Fig. 2) are 0.147275 d, 0.172157 d, 0.206914 d and 0.258718 d.

There is a clear difference between the short and the long period possibilities: while for the above two shorter periods (0.147275 d and 0.172157 d) the folded light curve is basically sinusoidal, it is double humped for the two longer periods. It is important to note that in both cases the primary minima have different brightnesses (differing by 0.2 mag).

For completeness we have also checked all other optical objects within the X-ray error circle for possible variability, but found no other variable star with an amplitude >0.2 mag down to 22 mag.

3. Spectroscopy

Low-dispersion spectroscopy has been performed on 1999 Jan. 22 with the EFOSC instrument at the 3.6m telescope on La Silla (ESO). A 300 grooves/mm grating has been used, giving a dispersion of 2.1 Å/pix and covering the wavelength range 3800–8000 Å. With the use of a 1.″5 slit (adapted to the seeing during that night) the FWHM resolution is 19 Å. The slit was oriented along the parallactic angle always. A total of seven consecutive spectra have been taken with exposure times of 1800 sec each except for the third spectrum with 2700 sec. Due to the faintness of the object and the suspected short orbital period the length of the exposures was a compromise between achieving a reasonable S/N ratio and minimizing the phase coverage of each exposure. One-dimensional spectra were extracted and processed using standard MIDAS routines. Wavelength calibration was done using He-Ar spectra taken before and after the sequence of spectra. The standard star GD108 was used for flux-calibration.

Table 2. He II λ4686 velocities (after subtraction of a systemic 346 km/s) and equivalent widths.

HJD mid-exposure	Velocity (km/s)	EW (Å)
2451201.11598	–49	4.8
.13757	–113	2.9:
.16525	+33	4.4
.20265	+123	3.9
.22424	+104	2.9
.24582	–11	3.8
.26741	–139	3.4

The spectrum of RX J0537.7–7034 has a steep, blue continuum and a moderately strong He II λ4686 emission line. The Balmer series appears in absorption except for Hα which seemingly is filled (Fig. 3). No other notable features are seen in the individual spectra. The phase-averaged sum of all spectra (Fig. 3) allows to identify a few other emission lines, among them He II λ4541, the C III/N III $\lambda\lambda$4630–4650 complex, and possibly also O VI λ5290.

Despite the low S/N of the individual spectra we attempted a measurement of the He II λ4686 line strengths and velocities. The result is given in Tab. 2 and plotted in Fig. 4. The He II λ4686 emission line shows a surprisingly clear radial velocity variation. Fitting a single sinusoidal curve yields a semiamplitude of $K = 115\pm20$ km/s and a

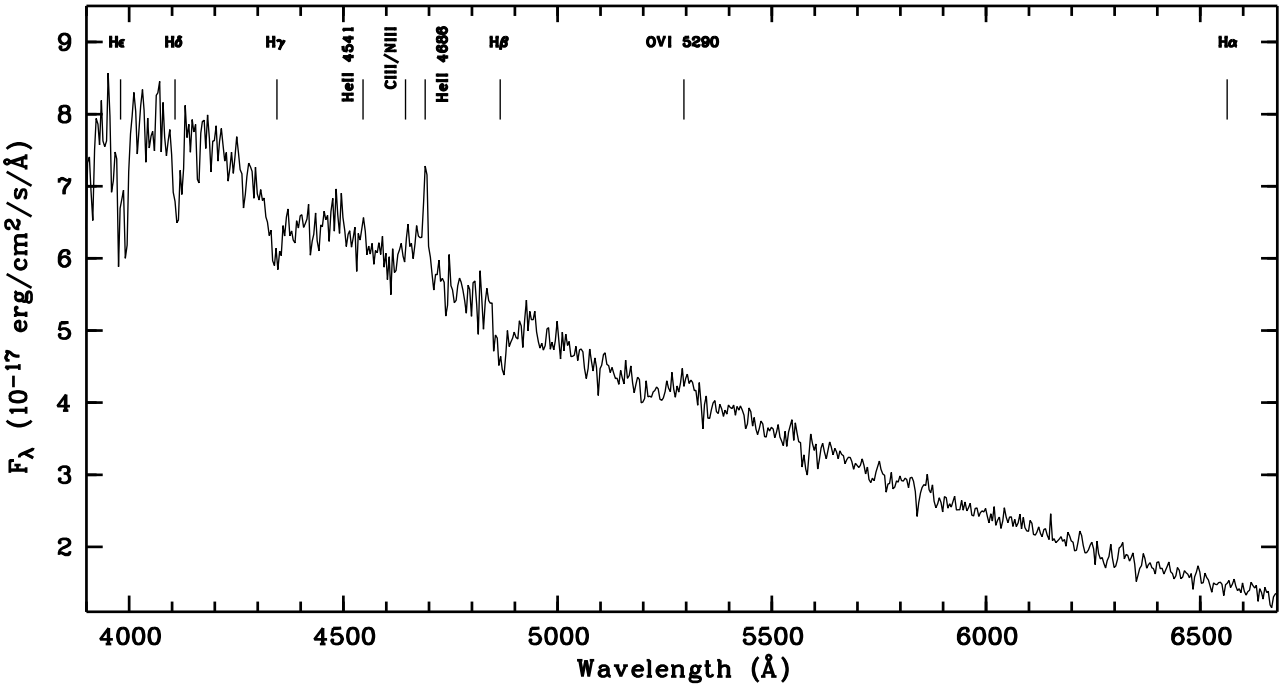

Fig. 3. Sum of all 7 spectra corresponding to an exposure time of 13 300 sec. The He II λ4686 emission line is prominent, and other detected lines are also marked. Note that the Balmer series is in absorption. With the present signal-to-noise ratio the existence of possible emission cores within the absorption troughs remains unclear.

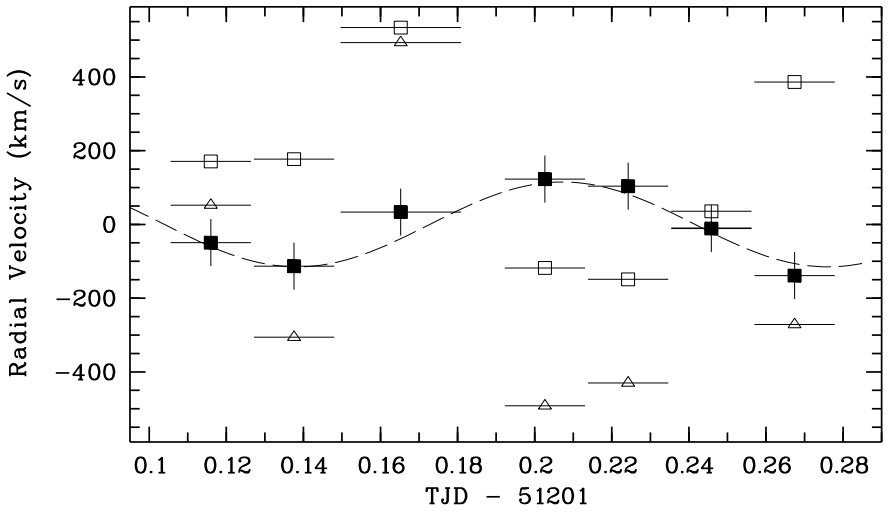

Fig. 4. Radial velocity curves of the He II λ4686 emission line (filled squares) and of the Hβ (open squares) and Hγ (open triangle) absorption lines as measured from the seven spectra taken in January 1999. The systemic velocity of 346 km/s has been subtracted. The emission line data are fitted with a sinusoidal curve (dashed line), resulting in a best-fit period of 3.3 hours. The velocity of the Balmer absorption lines seems not to be sinusoidal, and the amplitude is considerably larger than those of the He II line.

period of $P = 3.30 \pm 0.15$ hrs ($\chi^2_{\rm red} = 0.95$). The errors have been determined by a two-dimensional χ^2 fitting, i.e. the maximum and minimum possible periods have been determined for various values of the phase zero-point. If we use the standard procedure with a χ^2-minimization only along the y-axis (radial velocity), we get $K = 125 \pm 40$ km/s and a period of $P = 3.45 \pm 0.25$ hrs ($\chi^2_{\rm red} = 1.1$). The latter solution is plotted in the lower panel of Fig. 2. Though the errors for the spectroscopic period are large, the spectroscopic period matches one of our tentative photometric periods, namely the shortest one at 0.147275 d. We therefore adopt this value as the best orbital period, and the ephemeris for this is:

$$T = (2451203.6392 \pm 0.0040) + (0.147275 \pm 0.0038) \text{ days}$$

The photometric data of all 5 nights, folded with this period, are shown in Fig. 5. This demonstrates more clearly that while the light maxima have nearly identical brightnesses, the minima vary by slightly more than 0.2

Table 3. ROSAT X-ray observations of RX J0537.7–7034

Date	ROR	Detector	JD	count rate[(1)] (cts/s)	N_{cts}	HR1[(2)]
900616	120006p	PSPC	2448058.5	<0.0146		
900618	110169p	PSPC	2448060.5	<0.0121		
900619	110175p	PSPC	2448061.5	<0.0089		
900619-23	110176p	PSPC	2448063.5	<0.0079		
900621	110182p	PSPC	2448063.5	<0.0088		
900710	120101p	PSPC	2448082.5	<0.0131		
911129-1202	400079p[(3)]	PSPC	2448590.5	<0.0153		
920117-24	400079p[(3)]	PSPC	2448642.5	<0.0163		
920509-16	300172p	PSPC	2448755.5	0.0200±0.0020	92	–0.93±0.09
921218-26	300172p-1	PSPC	2448978.5	0.0178±0.0037	40	–0.83±0.16
930615-27	300172p-2	PSPC	2449159.5	<0.0049		
931215-6	300335p	PSPC	2449338.0	0.0044±0.0008	45	–1.00±0.15
940916	400352h	HRI	2449611.5	<0.0024		

(1) Upper limits are 2σ confidence, and for the PSPC observations have been calculated using only the soft channels 11–50.
(2) HR1 is the normalized count difference $(N_{52-201} - N_{11-41})/(N_{11-41} + N_{52-201})$, where N_{a-b} denotes the number of counts in the PSPC between channel a and channel b.
(3) The investigation of this pointed observation has been split for the present paper into the two distinct and widely separated temporal segments.

mag from one night to the other and to a somewhat lower degree even from one orbital cycle to the next (January 24 and 25, 1999). Also, the irregular brightness fluctuations are clearly visible.

Due to the uncertainty of our final period and the 2 day difference between spectroscopy and photometry we are unable to establish a relative phasing between radial velocity and intensity modulation.

Attempts to measure the absorption line velocities of Hβ and Hγ are very difficult due to both, the poor S/N and the possible distortion by emission cores (Hα is completely filled, and Hδ is at the very edge of our wavelength coverage). Nevertheless, it is obvious that these Balmer absorption lines exhibit a considerably larger velocity amplitude than the He II emission line (Fig. 4). Also, the velocity curve does not seem to be sinusoidal, and possibly out of phase with respect to He II λ4686. A formal (one-dimensional) fit of a circular orbit yields a period of 3.33 hrs, consistent within the errors to the He II emission line period.

4. Update of the X-ray light curve of RX J0537.7–7034

For the purpose of the discussion (see next paragraph) of alternative interpretations it seems useful to have the complete ROSAT X-ray light curve available. Though there has been no further ROSAT observation covering RX J0537.7–7034 since 1994 as presented in Orio et al. (1997), we have recalculated the count rates or upper limits, respectively, using the recently improved point spread function fitting and detection algorithms within the EXSAS package (Zimmermann et al. 1994). In addition, we used only PSPC channels 11–50 (corresponding to roughly 0.1–0.5 keV) for the upper limit calculation since the source in its on-state has such a very soft spectrum. Therefore, the intensity numbers of Tab. 3 differ slightly from those given by Orio et al. (1997). A visual representation of the table data is given in Fig. 6.

5. Discussion

5.1. Orbital variations and binary parameters

There are basically two different models to explain the optical orbital variations in supersoft X-ray binaries: (1) the optical light is produced by reprocessing of the white dwarf emission on the accretion disk, and the orbital variations are due to the varying aspect of the illuminated, heated, and flared accretion disk (Schandl et al. 1997); (2) these variations are due to the changing aspect of the irradiated secondary (van Teeseling et al. 1998). An irradiated secondary, if dominating the optical light, would produce a smooth, sinusoidal light curve. This indeed is what we observe on three out of the five nights. However, the irregular brightness variations and minima of different depths as well as the asymmetric minima during the two other nights are exactly what the flared accretion disk would produce when the accretion rate varies and the interaction of the accretion stream with the disk causes either a varying amount of "spray", e.g. matter splashing at the stream-disk impact site (Schandl et al. 1997) or a varying accretion disk rim height (Meyer-Hofmeister et al. 1997). Based on our available data we cannot distinguish between these two alternatives.

The origin of the He II emission line is still a mystery. If it came from the illuminated side of the donor, its radial velocity amplitude would have to be 300–400 km/s, much higher than the observed value of 115 km/s. Therefore, it

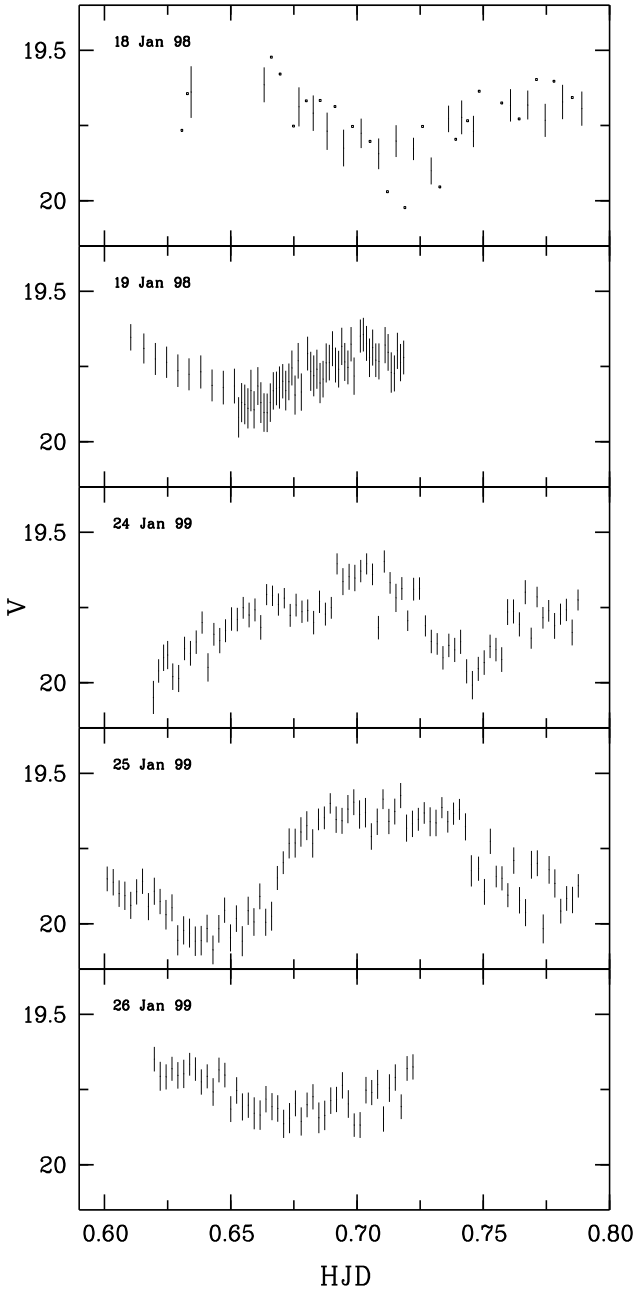

Fig. 1. V band light curves of RX J0537.7–7034 obtained during our 5 nights. The top panel includes in addition the B band data (filled squares) and the zero point of the x-axis is 0.05. Note the strong variability from night to night.

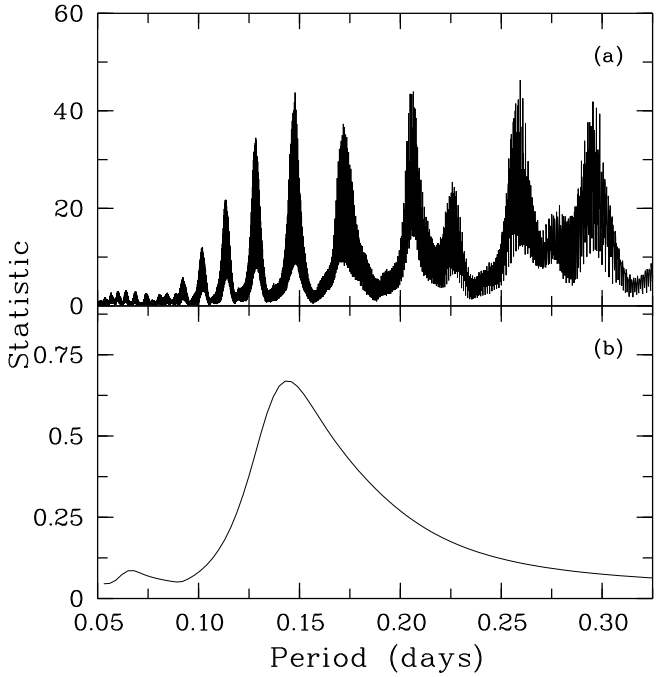

Fig. 2. Results of the period-search using the analysis-of-variance method for the photometry (top) and radial velocities (bottom). The adopted orbital period is that peak in the top panel which best coincides with the spectroscopic peak (0.147275 d).

is generally assumed that the He II emission line originates near to the accretor. Indeed, the expected velocity amplitude of the accretor (for our best period) is in the range 100–150 km/s.

If we assume that the measured He II emission-line velocity is roughly similar to the motion of the accretor, we may derive an estimate of the donor mass. Combining the orbital period and the velocity amplitude results in a mass function of f(M) = 0.023 ± 0.014 $M_\odot$. If we assume the donor to be a main-sequence star filling its Roche lobe, the resulting mass for the donor is restricted to a narrow range of 0.32–0.37 $M_\odot$, nearly independent of the inclination (Fig. 7).

The low mass of the donor implies that it does not contribute to the total light, since the apparent magnitude of a 0.35 $M_\odot$ star at the LMC distance is $m_V \sim 29$ mag. Thus, the optical emission as well as its orbital modulation must be caused differently, e.g. by the (irradiated) accretion disk. Also, it is very unlikely that the Balmer absorption lines arise in the illuminated secondary, unless the illumination increases the donor emission by 10 magnitudes. Since the white dwarf itself is also an unlikely source, we therefore tentatively assign the Balmer absorption lines to either the accretion disk or a possible wind. Substantially better data are needed to establish the velocity variations of the Balmer absorption lines, and thus shed more light on their nature.

The lack of detectable (at our accuracy) $B-V$ color variation through the orbital cycle of RX J0537.7–7034 suggests that the inner, bluer (hotter) part of the accretion disk are never occulted (during the 18 Jan. 1998 B band observation). This implies that the inclination is smaller than 70°–74°. Since RX J0537.7–7034 has shown luminous supersoft X-ray emission for the period of approximately one year, the white dwarf mass should be large enough to

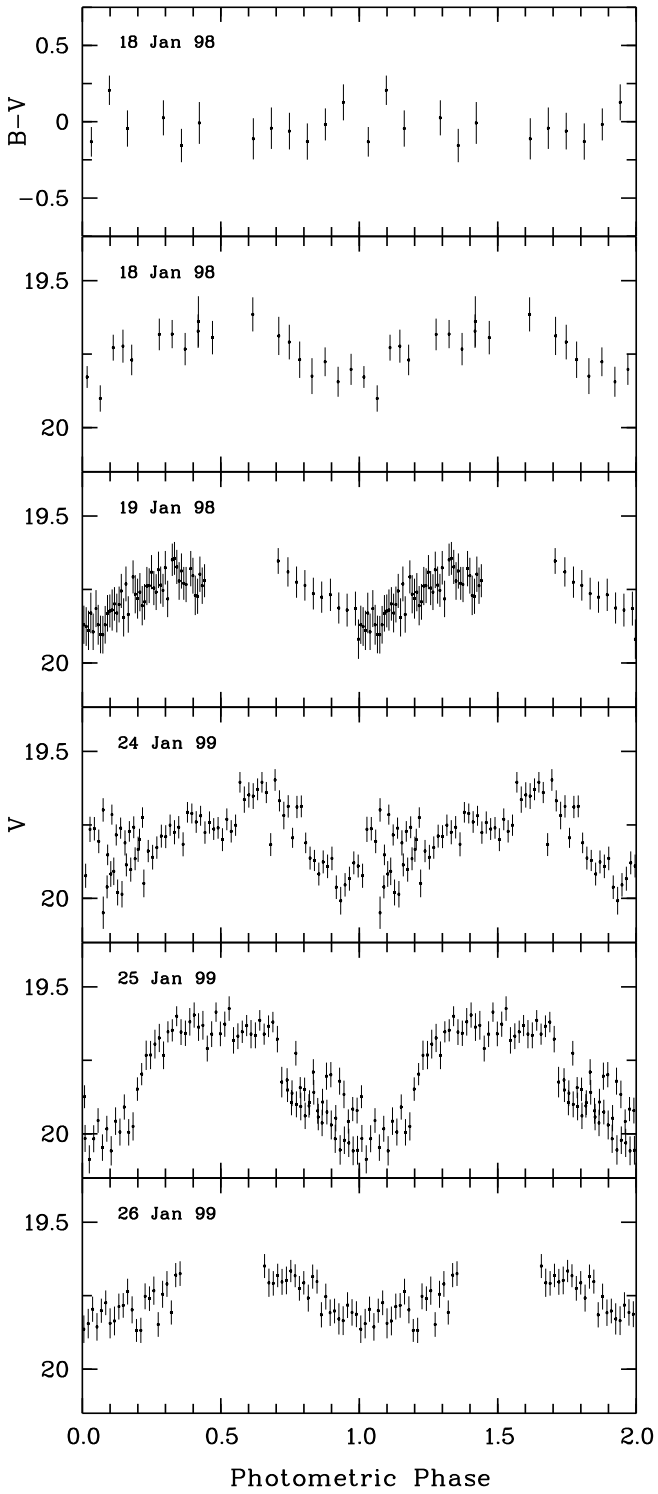

Fig. 5. Photometric data folded with the adopted period of 0.147275 d. The top panel shows $B-V$.

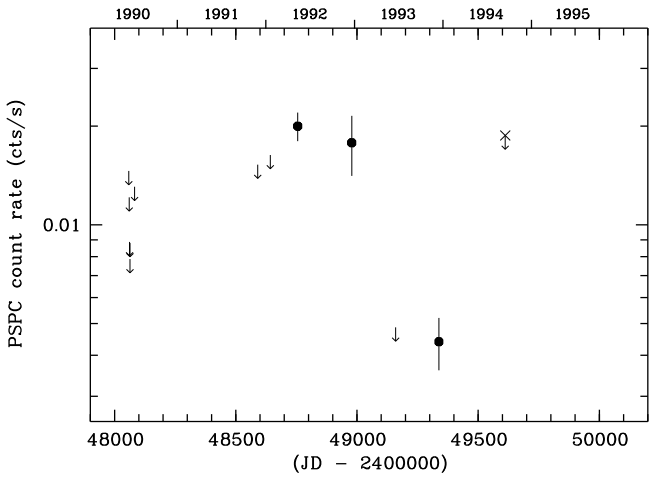

Fig. 6. X-ray light curve of RX J0537.7–7034 as observed with ROSAT. Arrows denote 2σ upper limits, and the HRI upper limit on HJD = 2449611 has been transformed into a PSPC count rate upper limit using the conversion factor 7.8 (Greiner et al. 1996).

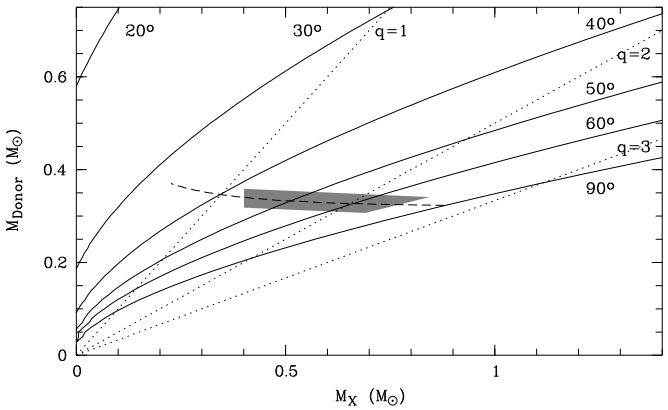

Fig. 7. Possible range of binary component masses based on our mass function of f(M)=0.023 $M_\odot$. Solid lines mark various inclinations of the binary plane, and dotted lines visualize constant mass ratio $q = M_{\rm X}/M_{\rm Donor}$. The dashed line indicates where the donor fills its Roche lobe (using the mass-radius relationship of Patterson 1984). The shaded area represents our best-estimate parameter space for the component masses (see text).

allow hydrogen burning. Previous investigations suggest a minimum mass of 0.4 $M_\odot$ (Sienkewicz 1980). This in turn implies (using Fig. 7) that the inclination should be >45 degrees. We therefore tentatively assume $i \sim 45°$–$70°$ in the following.

Since the inclination cannot be larger than 90 degrees, Fig. 7 also implies that the white dwarf mass is certainly smaller than 0.9 $M_\odot$. With the above best-estimate inclination range the mass of the white dwarf is < 0.8 $M_\odot$.

5.2. On the nature of RX J0537.7–7034

We have determined a period of ∼3.5 hrs for the supersoft X-ray source RX J0537.7–7034. Since this is a period in the range typically populated by (low-luminosity) cataclysmic variables it is worth mentioning here that the

systemic velocity of RX J0537.7–7034 of ∼350 km/s together with the characteristic spectrum of a SSS leaves no doubt that RX J0537.7–7034 is a supersoft X-ray source in the Large Magellanic Cloud, and not a galactic foreground cataclysmic variable. The lack of any other variable object within the X-ray error circle together with the improved X-ray position and the good positional match clearly suggest that the optical object studied here is indeed the optical counterpart of RX J0537.7–7034.

Many properties of RX J0537.7–7034 are very similar to those of SMC 13, a supersoft X-ray source in the Small Magellanic Cloud.. SMC 13 ≡ 1E 0035.4–7230 ≡ RX J0037.3–7214 (1RXS J003723.2–721415), has a 4.1 hrs orbital period (Schmidtke et al. 1996, Crampton et al. 1997, van Teeseling et al. 1998). In SMC 13 the Balmer absorption line system moves in phase with the He II emission lines, but with a larger amplitude. Based on the interpretation of the light curve as partially eclipsing (which constrains the inclination to $70^\circ < i < 78^\circ$) and the He II radial velocity data, Crampton et al. (1997) derive a donor mass of 0.4–0.5 $M_\odot$ and a mass of the accreting object of 1.3–1.5 $M_\odot$. In contrast, van Teeseling et al. (1998) interpret the orbital modulation by the varying aspect of the illuminated secondary, and derive an inclination of $20^\circ < i < 50^\circ$. Also, fitting non-LTE models to the BeppoSAX X-ray spectrum, Kahabka et al. (1999) derive a white dwarf mass of 0.6–0.7 $M_\odot$ consistent with the inclination range of van Teeseling et al. (1998). Thus, RX J0537.7–7034 shares the following characteristics with SMC 13: (i) the short orbital period, (ii) an almost identical optical spectrum, (iii) the existence of Balmer absorption lines, (iv) the different velocities of He II emission and Balmer absorption lines, (v) the low visual absolute magnitude (see Tab. 4). (vi) the luminous, soft X-ray spectrum, and (vii) possibly a low white dwarf mass. But there is also one clear difference: RX J0537.7–7034 shows a factor of 7 X-ray variability over the past 8 years while 1E 0035.4–7230 has been completely constant (e.g. Kahabka et al. 1999).

With $P_{\rm orb} \sim 3.5$ hrs RX J0537.7–7034 is the shortest-period binary among the SSS. This implies that the standard scenario of SSS, in which the donor is assumed to be more massive than the accreting white dwarf to ensure high mass transfer rates on a thermal timescale (van den Heuvel et al. 1992), is not applicable for this system. Under the assumption of Roche-lobe filling and a minimum white dwarf mass for steady-state burning of ∼0.5–0.6 $M_\odot$ (Fujimoto 1982, Sion & Starrfield 1994, Cassisi et al. 1998), a mass ratio $q \equiv M_{\rm Donor}/M_{\rm WD} > 1$ implies that $P_{\rm orb} \gtrsim 4.5-5$ hours always. In addition, with a donor mass of about 0.35 $M_\odot$ it seems impossible to have a less massive white dwarf with H burning. Thus, RX J0537.7–7034 clearly does not fit this standard scenario.

Similar arguments, though not as strong (because the component parameters are less constrained), have been put forward for SMC 13 (Crampton et al. 1997). Thus, there are now two sources which require a new donor scenario. Alternative scenarios are either symbiotic systems (see Kahabka & van den Heuvel 1997), classical novae (e.g. Ögelman et al. 1993), the systems that Kahabka and Ergma (1997) define "SMC 13" type, and wind-driven binaries (van Teeseling & King 1998). Symbiotics, involving giant donors, have much too long orbital periods to be applicable to RX J0537.7–7034. A classical post-nova interpretation (similar to e.g. GQ Mus; Ögelman et al. 1993) is also unlikely since the LMC was continuously monitored to search for novae in the last 50 years, and a novae would have been detected in the optical passband. Thus, there are two serious alternative explanations for RX J0537.7–7034:

1. SMC 13 systems: SMC 13 is interpreted by Kahabka & Ergma (1997) as a cataclysmic variable with a low mass white dwarf (0.6–0.7 $M_\odot$ white dwarf) having a thick helium buffer layer. Such a system must have been a classical nova in which, after a number of outbursts, the white dwarf was heated up. As a consequence the flashes have become very mild, without actual mass loss, and the system is proposed to presently be in a phase of residual hydrogen burning after a mild shell flash. Van Teeseling & King (1998) have argued on statistical grounds that such a phase should last longer than 100 yrs. In order for the residual burning to last long enough (at least about 20 years since the *Einstein* discovery; Seward & Mitchell 1981), a low CO abundance of the burning matter and a hot, low-mass (0.6–0.7 $M_\odot$) white dwarf are required. Sion & Starrfield (1994) have demonstrated that hot white dwarfs with masses as low as 0.5 $M_\odot$ can stably burn hydrogen in a steady state.
2. wind-driven binaries: Van Teeseling & King (1998) have shown that the strong X-ray flux in supersoft

Table 4. Comparison of brightness and colours of SSS. We assume here 18.5 mag as the distance modulus for the LMC (Panagia et al. 1991), 18.8 mag for the SMC and reddening E(B-V)=0.065 and E(B-V)=0.043 for the LMC and SMC, respectively.

SSS	P (d)	$M_{\rm V}$	B–V	U–B	Refs.[1]
CAL 83	1.04	–1.3	–0.06		1, 2
CAL 87	0.44	+0.1	+0.1		3
RX J0537.7–7034	0.14	+1.0	–0.03	–0.69	4, 5
SMC 13	0.17	+1.4	–0.13	–1.13	6, 7, 8
RX J0439.8–6809	0.15?	+2.9	–0.2	–1.25	9, 10
GQ Mus[2]	0.06	+2.7	–0.3	–1.1	11

[1] References: (1) Crampton et al. (1987), (2) Smale et al. (1988), (3) Schmidtke et al. (1993), (4) Orio et al. (1997), (5) this work, (6) Schmidtke et al. (1996), (7) Crampton et al. (1997), (8) van Teeseling et al. (1998), (9) Schmidtke & Cowley (1996), (10) Teeseling et al. (1996), (11) Diaz & Steiner (1989)
[2] During the phase as a supersoft X-ray source.

sources should excite a strong wind ($\dot{M}_{\rm wind} \sim 10^{-7}$ $M_\odot$/yr) from the irradiated companion which in short-period binaries would be able to drive Roche lobe overflow at a rate comparable to $\dot{M}_{\rm wind}$. This may self-consistently sustain stable recurrent or steady-state hydrogen burning on the white dwarf. In binaries with a low-mass companion, the angular momentum loss by the wind may dominate the binary evolution, and cause the period to increase with time. One important open question of this scenario is how a system could eventually enter such a self-consistent wind-driven phase. Van Teeseling & King (1998) suggested either a preceding SMC 13 phase, or a late helium shell flash of the cooling white dwarf after the binary has already come into contact as a cataclysmic variable.

Because of the X-ray variability of RX J0537.7–7034 its secure classification into one of the above two scenarios seems difficult. One could expect that the SMC 13 systems should display a rather smooth X-ray light curve, unless a mild flash is occurring. Such a flash should be accompanied by some optical brightening, however. Also, if the X-ray turn-off of RX J0537.7–7034 were to be explained by an only short phase (∼1 year as observed) of burning, the white dwarf mass must be high (>1.1 $M_\odot$), contrary to our findings (see Fig. 7). Finally, the residual burning (between the H flashes) should be connected to a temperature increase (Sion & Starrfield 1994), while the observations tend to suggest the opposite behaviour (see the hardness ratio values in Tab. 3 which are softest ≡ coolest during the last detection).

Whether or not the wind-driven supersoft source scenario is valid, remains to be seen: (i) The drop in X-ray intensity in 1993 is very probably not caused by increased absorption in the wind, otherwise the sensitive hardness ratio HR1 would have changed substantially; (ii) since it is difficult to enter the self-excited wind phase, any repeated on-states would be hard to explain – assuming that the observed X-ray decline corresponds to the sudden end of this wind-driven phase; (iii) this phase would have lasted less than two years (Fig. 6) – was it just an unsuccessful attempt to enter the wind-driven phase? Overall, the wind-driven supersoft source scenario seems to provide a possible explanation for RX J0537.7–7034, though it remains unclear what the observational consequences would be.

6. Conclusions

We have obtained new photometric and spectroscopic data of the supersoft X-ray source RX J0537.7–7034 which show that

1. the orbital period is ∼3.5 hrs,
2. the inclination of the orbital plane is $45° \lesssim i \lesssim 70°$,
3. the component masses are $0.4 \lesssim M_{\rm accretor} \lesssim 0.8$ $M_\odot$ and $0.32 \lesssim M_{\rm donor} \lesssim 0.37$ $M_\odot$, respectively,
4. the canonical scenario of thermal-timescale mass transfer from a donor more massive than the white dwarf (van den Heuvel et al. 1992) is clearly not applicable,
5. the binary system RX J0537.7–7034 could be a SMC 13 system or wind-driven system, though the observed X-ray variability poses problems for both scenarios.

RX J0537.7–7034 is still quite puzzling in many respects, and new observations at different wavelengths should help solving the riddle. The important and exciting fact is that it is a new type of transient X-ray source, possibly representative of a whole new class, and understanding it will also add to a better understanding of close binary evolution.

Acknowledgements. JG and RS are supported by the German Bundesministerium für Bildung, Wissenschaft, Forschung und Technologie (BMBF/DLR) under contract Nos. FKZ 50 QQ 9602 3 and 50 OR 9708 6, and MO by the Italian Space Agency Research Program.

References

Cassisi S., Iben I.Jr., Tornambe A., 1998, ApJ 496, 376
Crampton D., Cowley A.P., Hutchings J.B., et al. 1987, ApJ 321, 745
Crampton D., Hutchings J.B., Cowley A.P., Schmidtke P.C., 1997, ApJ 489, 903
Diaz M.P., Steiner J.E., 1989, ApJ 339, L41
Fujimoto M.Y., 1982, ApJ 257, 767
Greiner J. (Ed.), 1996, Supersoft X-ray Sources, Lect. Notes in Physics 472, Springer
Greiner J., Schwarz R., Hasinger G., Orio M., 1996, A&A 312, 88
Kahabka P., Ergma E., 1997, A&A 318, 108
Kahabka P., van den Heuvel E.P.J., 1997, ARAA 35, 69
Kahabka P., Parmar A.N., Hartmann H.W., 1999, A&A 346, 453
Landoldt A.U., 1992, AJ 104, 340
Long K.S., Helfand D.J., Grabelsky D.A., 1981, ApJ 248, 925
Mateo M., Schechter P., 1989, in *1st ESO/ST-ECF Data Analysis Workshop* eds. P.J. Grosbol, F. Murtagh & R.H. Warmels, p. 69
Meyer-Hofmeister E., Schandl S., Meyer F., 1997, A&A 321, 245
Motch C., Werner K., Pakull M.W., 1993, A&A 268, 561
Ögelman H., Orio M., Krautter J., Starrfield S., 1993, Nat. 361, 331
Orio M., Ögelman H., 1993, A&A 273, L56
Orio M., 1995, in "Cataclysmic Variables", eds. A. Bianchini, M. Della Valle and M. Orio, Dordrecht Boston: Kluwer Academic Publishers, p. 429
Orio M., Della Valle M., Massone G., Ögelman H., 1997, A&A 325, L1
Pakull M.W., Beuermann K., Angebault L.P., Bianchi L., 1987, Ap&SS 131, 689
Pakull M.W., Beuermann K., van der Klis M., van Paradijs J., 1988, A&A 203, L27
Panagia N., Gilmozzi R., Macchetto F., Adorf H.-M., Kirshner R.P., 1991, ApJ 380, L23
Patterson J., 1984, ApJS 54, 443

Rappaport S., DiStefano R., Smith J.D., 1994, ApJ 426, 692
Schandl S., Meyer-Hofmeister E., Meyer F., 1997, A&A 318, 73
Schmidtke P.C., McGrath T.K., Cowley A.P., Frattare L.M., 1993, PASP 105, 863
Schmidtke P.C., Cowley A.P., 1996, AJ 112, 167
Schmidtke P.C., Cowley A.P., Mc Grath T.K., Hutchings J.B., Crampton D., 1996, AJ 111, 788
Schwarzenberg-Czerny A., 1989, MNRAS 241, 153
Seward F.D., Mitchell M., 1981, ApJ 243, 736
Sienkewicz R., 1980, A&A 85, 295
Sion E.M., Starrfield S.G., 1994, ApJ 421, 261
Smale A.P., Corbet R.H., Charles P.Q., et al., 1988, MNRAS 233, 51
van den Heuvel E.P.J., Bhattacharya D., Nomoto K., Rappaport S.A., 1992, A&A 262, 97
van Teeseling A., King A.R., 1998, A&A 338, 957
van Teeseling A., Reinsch K., Beuermann K., 1996, A&A 307, L49
van Teeseling A., Reinsch K., Hessman F.V., Beuermann K., 1997, A&A 323, L41
van Teeseling A., Reinsch K., Pakull M.W., Beuermann K., 1998, A&A 338, 947
Wang Q., 1991, MNRAS 252, 47p
Zimmermann H.U., Becker W., Belloni T., Döbereiner S., Izzo C., Kahabka P., Schwentker O., 1994, MPE report 257